

The Stability of Nodal Points in the Leveling Network in the Southwest Part of Israel

Gilad EVEN-TZUR, Israel

Key words: leveling, deformation, GPS, datum

SUMMARY

Repeated precise leveling surveys carried during the past decade point to an instability of the nodal points in the leveling network in the southwest part of Israel. This situation prevents the adjustment of the leveling network properly which would ensure the providing of correct heights for benchmarks. Modeling the regional and the local vertical movement of points will enable adjustment of the leveling network, which contains lines that were measured in different times.

For the purpose of monitoring the stability of nodal points nine GPS campaigns were carried in the region over a period of one calendar year. In this study the large number of monitoring sessions enabled the investigation of the fluctuations of the nodal points, based on physical processes such as the cyclic effects of swelling and shrinking of the ground.

The GPS measurements were analyzed by a Two-Step analysis. In the first step the geodetic measurements were processed sequentially without modeling the variations in the height of the networks points. In the second step the variations in the network geometry were modeled by means of a physical model.

The Stability of Nodal Points in the Leveling Network in the Southwest Part of Israel

Gilad EVEN-TZUR, Israel

1. INTRODUCTION

Nodal points of a leveling network are used as a basis to determine the heights of benchmarks in the national vertical control network. Repeated precise leveling surveys during the past decade pointed to an instability (of up to several cm) of the nodal points in the leveling network in the southwest part of Israel. This renders any attempts for a network adjustment to failure. In order to examine the behavior of the nodal benchmarks intensive monitoring measurements were carried using GPS. The goal of the monitoring network is two-fold, to estimate the model of any vertical motion of the benchmarks and to define areas in the network which behave in a similar way. Multiple monitoring sessions over a period of a year provided the ability to monitor global and seasonal behavior of the nodal benchmarks.

The vertical accuracy of GPS measurements is not in the same quality of the leveling measurements, but they are relatively inexpensive and fast. These advantages enable the measuring of monitoring network several times a year. Since the previous leveling campaigns in the investigated area pointed to vertical movements of several centimeters, the GPS measurements enabled the monitoring of these movements.

This paper describes the design of the monitoring network and the GPS measurement process. It presents the analysis of the monitoring network using a Two-Steps analysis, based on two deformation models which describe the vertical position of a point relative to time, the linear motion model and the swelling and shrinking dynamic model.

2. THE METHOD OF TWO-STEPS ANALYSIS

Two types of models are pertinent in deformation analysis, the mathematical model that represents the geodetic measurements and the deformation model. The mathematical model is usually conceived as being absolutely correct, while the measurements are regarded as quantities corrupted by measurement noise. The deformation model should describe the physical reality, but the validity of the physical model and its system noise is frequently limited.

Estimation of the deformation parameters directly from the geodetic measurements may lead to undesirable results. System noise due to inadequacies of the physical model may cause sever distortions of the parameter estimates.

The relationship between a vector of measurements ℓ and a vector of parameters \mathbf{x} can be expressed by a set of observation equations, given as:

$$\ell = \mathbf{Ax} + \mathbf{v} \quad (1)$$

\mathbf{A} denotes the Jacobian matrix and \mathbf{v} is the measurement noise vector. It may be assumed that \mathbf{A} is a column rank deficient due to the need for datum definition. The parameters \mathbf{x} are

calculated under the minimum condition $\mathbf{v}^T \mathbf{P} \mathbf{v}$, where \mathbf{P} is the weight matrix of the observations.

Since the vector of parameters \mathbf{x} can be expressed as a linear function of a vector of parameters \mathbf{s} , another set of equations may be created:

$$\mathbf{x} = \mathbf{B}\mathbf{s} + \mathbf{w} \quad (2)$$

where \mathbf{B} denotes the Jacobian matrix and is usually a full column rank matrix, and \mathbf{w} is the model noise vector. The parameters \mathbf{s} are calculated under the minimum condition $\mathbf{w}^T \mathbf{P}_x \mathbf{w}$, where \mathbf{P}_x is the weight matrix of the observations in the second model.

This approach for solving \mathbf{s} indirectly from the measurements vector ℓ while using a vector of pseudo-measurements \mathbf{x} is referred to as a Two-Step analysis (Papo and Perelmuter, 1993), where in the first step \mathbf{x} is solved using the measurement vector ℓ , and in the second step \mathbf{x} is used as pseudo-measurements for solving the parameter vector \mathbf{s} .

Substituting equation (2) into equation (1) yields the One-Step analysis:

$$\ell = \mathbf{A}(\mathbf{B}\mathbf{s} + \mathbf{w}) + \mathbf{v} = \mathbf{A}\mathbf{B}\mathbf{s} + \mathbf{A}\mathbf{w} + \mathbf{v} \quad (3)$$

where the measurements vector ℓ consists of a systematic part $\mathbf{A}\mathbf{B}\mathbf{s}$, and two random parts $\mathbf{A}\mathbf{w}$ and \mathbf{v} .

This paper employs the Two-Steps analysis method for monitoring the stability of nodal points in the leveling network in the southwest part of Israel.

For k sets of measurements ℓ_i , each vector of parameters \mathbf{x}_i can be estimated independently as:

$$\hat{\mathbf{x}}_i = (\mathbf{A}_i^T \mathbf{P}_i \mathbf{A}_i)^{-1} \mathbf{A}_i^T \mathbf{P}_i \ell_i \quad (4)$$

with the attached cofactor matrix $\mathbf{Q}_{\hat{\mathbf{x}}_i} = (\mathbf{A}_i^T \mathbf{P}_i \mathbf{A}_i)^{-1}$ and the variance-covariance matrix $\Sigma_{\hat{\mathbf{x}}_i} = \hat{m}_{0i}^2 \mathbf{Q}_{\hat{\mathbf{x}}_i}$, where $\hat{m}_{0i}^2 = \frac{\hat{\mathbf{v}}_i^T \mathbf{P}_i \hat{\mathbf{v}}_i}{r_i}$, and r_i is the adjustment redundancy. The estimated

solution vector $\hat{\mathbf{x}}^T = [\hat{\mathbf{x}}_1 \quad \hat{\mathbf{x}}_2 \quad \dots \quad \hat{\mathbf{x}}_k]^T$ resulting from the first step will be used as pseudo-measurements in the second step.

The set of deformation model parameters $\hat{\mathbf{s}}$ is solved by equation (2) (Papo and Perelmuter, 1993):

$$\hat{\mathbf{s}} = (\mathbf{B}^T \mathbf{P}_x \mathbf{B})^{-1} \mathbf{B}^T \mathbf{P}_x \hat{\mathbf{x}}, \quad (5)$$

The weight matrix \mathbf{P}_x is produced by using the variance-covariance matrix $\Sigma_{\hat{\mathbf{x}}}$ instead of the cofactor matrix $\mathbf{Q}_{\hat{\mathbf{x}}}$ (Even-Tzur, 2003). The cofactor matrix $\mathbf{Q}_{\hat{\mathbf{s}}}$ and the variance-covariance matrix $\Sigma_{\hat{\mathbf{s}}}$ are:

$$\mathbf{Q}_{\hat{\mathbf{s}}} = (\mathbf{B}^T \mathbf{P}_x \mathbf{B})^{-1}; \quad \Sigma_{\hat{\mathbf{s}}} = \hat{m}_0^2 \mathbf{Q}_{\hat{\mathbf{s}}} \quad (6)$$

While \hat{m}_0^2 is equal to (Even-Tzur, 2003):

$$\hat{m}_0^2 = \frac{\sum_{i=1}^k r_i + \mathbf{w}^T \mathbf{Q}_x^{-1} \mathbf{w}}{\sum_{i=1}^k r_i + r_{II}} \quad (7)$$

3. NETWORK DESIGN AND FIELD DATA COLLECTION

The monitoring network contained 10 points. Preference was given to nodal benchmarks existing in the leveling network, but some nodal points were destroyed over the years and nearby benchmarks were selected instead. Some of the nodal points in the investigated area were not suitable for GPS measurements but the chosen benchmarks were ones established with good geotechnical standards. Benchmarks without suitable stability, for example ones that were located on electric poles or bridges, were disqualified. Three points from the Israeli Geodetic-Geodynamic network were also chosen. These points were built according to high technical specifications to ensure their geotechnical stability (Karcz, 1994) and it is important to monitor their stability. After considerations of the requirements, conditions and constraints, and after a tour in the field ten benchmarks were chosen, (the locations can be seen in figure 2 and their construction methods are detailed in table 1. An additional permanent GPS station located in the investigated area was added to the network.

For vertical movement monitoring purposes the GPS antenna set-up is of great importance. To increase the reliability of the network a GPS antenna was set up twice, independently, at each point in order to detect and identify gross errors resulting from the positioning of the GPS antenna at the marker points, identify alignment errors, and measure the antenna height.

Four Trimble dual frequency GPS receivers (3×4000SSE and 1×4000SSI) with geodetic antennas were used for the network measurements. The antennas were set up on tripods except at the G1 points, where a special device that was screwed to the point and enabled a stable set up of the GPS antenna for long periods of time was used.

Five sessions enabled measuring the network with two independent antenna set ups in each point. The duration of each session was planned for 4.5 hours. In each campaign the same sessions were measured.

Name	Location	Construction
718/A	Port of Ashdod	Bolt on concrete banister on platform
402U	Ashqelon Marina	Bolt on concrete banister on platform
65/F	Southern exit of Yavne	Bolt on solid rock
40/F	Pelugot junc.	8 m drilling pipe
362/A	Urim junc.	4 m drilling pipe
436/A	Northern to Omer	4 m drilling pipe
4727	Qama junc.	Wall nail on concrete banister
EZRA	Ezricam junc.	4.5 m drilling pipe (G1)
ASHK	Southeast to Ashkelon	4.5 m drilling pipe (G1)

Name	Location	Construction
OFKM	Park of Ofaqim	4.5 m drilling pipe (G1)
LHAV	Kibbutz Lahav	5 drilling pipes to depth of 4 m. (permanent GPS site)

Table 1: The network BM location and method of construction.

4. FIRST STEP: EPOCH BY EPOCH DATA PROCESSING

Each session was processed with the permanent GPS site (LHAV). Every processing contained five sites, which enabled the production of 10 baselines. The coordinates of the permanent GPS station were set as fixed in each session processing. Solutions were determined using the linear combination method and a value of 15 degrees was used as the default cutoff elevation angle for all the processing. The sessions were processed using precise orbits, as disseminated by the International GPS Service (IGS). The average vector length was 27 km, while the longest vector was 55 km long.

The baselines were adjusted into a network, while the 3×3 variance-covariance matrix associated with each baseline was used for weighing the observations. To ensure that the error model would match the GPS observations better, the variance-covariance matrix was multiplied by a constant scale factor.

Detection of gross errors was performed using the w-test. Gross errors in the adjusted model will result in the reduction of the quadratic form of the residuals ($\hat{v}^T P \hat{v}$) by (Chen, 1987 and Etrog, 1991):

$$\Delta R = \hat{v}^T P E (E^T P Q_v P E)^{-1} E^T P \hat{v}, \quad (8)$$

while Q_v is the Least Squares estimation of the residuals cofactor matrix and E is a matrix with the same number of columns as the number of suspected outliers, n_2 , with a unit value in the row which correlates to the suspicious observation and zeros in all other rows. The test statistic is $\Delta R / n_2 \sigma_0^2 \sim F_{\alpha, n_2, \infty}$, where α is the significance level and σ_0^2 is the a-priori variance factor. When the observations in the Least Squares adjustment are GPS vectors the E matrix contains 3 times the number of columns, since each vector contains three components.

For j receivers there are $j(j-1)/2$ single vectors, while only $j-1$ of these vectors are independent. We therefore multiply the normal matrix by factor $2/j$ to compensate for the artificial increase of redundancy resulting from the use of all possible vectors (Han and Rizos, 1995).

The network contained 11 points. Five sessions were measured in each monitoring epoch which included 5 sites (except the last monitoring epoch, where one session was measured twice). Ten vectors were processed from each session, in total 50 vectors per monitoring epoch. The number of unknown parameters to be solved was 30 ($3 \times 11 - 3$), and the number of observation equations was 150, so for the sum of 120 degrees of freedom could be expected in the adjustment process. The degrees of freedom are reduced by 3 for each vector that is removed from the system. The results of the data processing for each session can be seen in table 2.

Estimations of the accuracy of the network points in a local horizon system in the free net solution for all 9 monitoring epochs can be seen in table 3. These values present the accuracy of the measurements without any influence of outside factors such as datum definition.

The accuracy of LHAV is significantly higher than that of the other points. Including LHAV in every session processing dramatically increased the number of local degrees of freedom, this which resulted in a higher accuracy. In the G1 points a special device that was screwed to the point and enabled a stable set-up of the GPS antenna for long periods of time was used, while all the other points were measured using a tripod. However, it can not be claimed that using the special devise for the GPS antenna set-up improved the accuracy compared to points that were measured by tripod.

Monitoring number	Average GPS day	Number of days between sequential monitoring	Factor	Degrees of freedom	\hat{m}_0^2
1	011-2002	0	5	117	1.041
2	067-2002	56	5.5	120	0.932
3	127-2002	60	6	120	1.003
4	162-2002	35	7	117	1.039
5	211-2002	49	5.5	111	0.940
6	246-2002	35	8	108	0.983
7	296-2002	50	8	114	1.071
8	345-2002	49	8	120	1.014
9	038-2003	58	8	135	1.011

Table 2: Summery of the nine monitoring campaigns.

Point name	Accuracy (1σ)		
	average [m]	minimum [m]	maximum [m]
LHAV	0.0046	0.0036	0.0073
436A	0.0075	0.0054	0.0103
659U	0.0069	0.0049	0.0096
OFKM	0.0067	0.0049	0.0093
073U	0.0069	0.0048	0.0106
ASHK	0.0058	0.0045	0.0083
402U	0.0062	0.0051	0.0088
040F	0.0074	0.0054	0.0104
065F	0.0063	0.0043	0.0098
406U	0.0058	0.0044	0.0089
EZRA	0.0057	0.0043	0.0091

Table 3: The accuracy of the network points in a local horizon system in the free net solution.

5. SECOND STEP: DEFORMATION ANALYSIS

The minimum constraints solution of the network points height for each monitoring epoch and their variance-covariance matrix are used as pseudo-measurements for the solution of the Second Step, where in each solution different models can be tested to describe the vertical position of the network points.

5.1 The Deformation Model

Two deformation models were tested to describe the vertical position of a point relative to time, the linear motion model and the swelling and shrinking dynamic model. The height of a point h in time t is described in the linear model as equal to

$$h = h_0 + \dot{h}\Delta t \quad (9)$$

where h_0 is the vertical location of the point in standard time t_0 , \dot{h} is the linear velocity of the point and $\Delta t = t - t_0$.

In the dynamic model a cyclic factor is added for the description of the vertical position. The model represent the vertical location relative to time is received from the integration of the dynamic model describing the acceleration \ddot{h} of a point:

$$\ddot{h} = \frac{2\pi \cdot c}{T} \cos\left(\frac{2\pi}{T} \Delta t\right) \quad (10)$$

It is a simple sinusoidal model which is dependant on the coefficient c representing the swelling/shrinking. The cycle period is T , and the acceleration is calculate for time t_i relative to the reference time t_0 , where $\Delta t = t_i - t_0$. The vertical height of a point as derived from the integration of equation 10 is

$$h = h_0 + \dot{h}\Delta t - \frac{cT}{2\pi} \cos\left(\frac{2\pi}{T} \Delta t\right) \quad (11)$$

where the three parameters, h_0 , \dot{h} and c are unknowns and should be solved.

5.2 The Statistical Tests

Statistical tests are applied for estimating the correspondence of the motion model and its significance. Parameter \underline{x} that is derived from the measurements is tested to see if it is significantly different from parameter x with a certain confidence level $(1 - \alpha)$. The null hypothesis (H_0) is tested against any alternative hypothesis (H_1):

$$\begin{aligned} H_0 : \underline{x} &= x \\ H_1 : \underline{x} &\neq x \end{aligned} \quad (12)$$

When only one parameter is tested the Chi Square (χ^2) distribution is used, and when a vector of parameters is tested the Fisher (F) distribution (Cooper, 1987) is used. When \underline{Q}_x is the cofactor matrix of \underline{x} , the null hypothesis is tested against the alternative hypothesis using the value w obtained from Equation (13) (Hamilton, 1964, Koch, 1999):

$$w = [(\underline{\mathbf{x}} - \mathbf{x})^T \underline{\mathbf{Q}}_x^{-1} (\underline{\mathbf{x}} - \mathbf{x})] / d. \quad (13)$$

The calculated value w is tested against $F(\alpha, h, r)$, which is determined based on the Fisher distribution with the chosen significance level α , the degrees of freedom r , and d the rank of $\underline{\mathbf{Q}}_x$. The null hypothesis is rejected if $w > F(\alpha, r, d)$.

5.3 Results

5.3.1 The linear motion model

The free net solution of the linear motion model showed an a-posteriori variance factor of unit weight equaling $\hat{m}_0^2 = 1.066$, while the model noise was $\mathbf{w}^T \mathbf{P}_x \mathbf{w} = 152.0$. The ratio between the a-posteriori variance factor and the a-priori variance factor ($m_0^2 = 1.0$) is tested. The test statistic is (Cooper, 1987)

$$\Omega = \frac{\hat{m}_0^2}{m_0^2} \square F(\alpha, r, \infty). \quad (14)$$

The 9 sessions provided 1128 degrees of freedom, a rather high value in the assessment of s , meaning that r can be defined as infinity, $r = \infty$. A failure of the test might be caused by an incompatible model, gross errors or a weighting problem. The test is accepted if $\Omega < F$. Setting the significance level at $\alpha = 5\%$ for the linear model resulted in $F(5, 1128, \infty) = 1.07$, and the test was accepted, marginally.

At the second step, the velocity ($\dot{\mathbf{h}}$) of the network points was tested. The null hypothesis $H_0 : \dot{\mathbf{h}} = 0$ was tested against the alternative hypothesis $H_1 : \dot{\mathbf{h}} \neq 0$. As the dimension of \mathbf{P}_x equaled 11×11 and its defect was 1, the rank of the matrix was $d = 10$. Thus $F(5, 10, \infty) = 1.83$ was obtained for an $\alpha = 5\%$ level of accuracy. According to Equation (13) $w = 1.40$. Since $w < F$ the null hypothesis was accepted, at a significance level of $\alpha = 5\%$, signifying that there was no linear movements during the measurement campaigns.

5.3.2 The swelling and shrinking model

The cycle period $T = 1$ was set for testing a yearly cycle. When setting $t_0 = 2002.1$, a minimum model noise equaling $\mathbf{w}^T \mathbf{P}_x \mathbf{w} = 101.4$ was received for the zero epoch.

The a-priori variance factor was $\hat{m}_0^2 = 1.031$. It is obviously clear that this dynamic model better fits the observations than the linear motion model. The $\dot{\mathbf{h}}$ and $\dot{\mathbf{c}}$ were tested for the \mathbf{P}_x dimension of 22×22 and its defect 2, and the rank of the matrix was $d = 20$. When setting an $\alpha = 5\%$ level of significance, $F(5, 20, \infty) = 1.57$ was obtained. $w = 3.15$ was calculated according to Equation (13). Since $w > F$ the null hypothesis was rejected at the significance level $\alpha = 5\%$, indicating that swelling and shrinking movements occurred during the measurement campaigns.

To clarify which points moved a datum had to be defined. An S-transformation was applied to transform vector s and its covariance matrix to a weight constraints solution. Congruency testing was performed to determine the stable datum points (as presented in Equation (13)) but the test statistic was applied only to the datum points.

Five points (362A, OFKM, 4727, 402U, 040F) in the center of the network were selected as datum (see Fig. 2). For an $\alpha = 5\%$ level of significance, $F(5,8,\infty) = 1.94$ was obtained. According to Equation (13) $w = 0.63$ was obtained. Since $w < F$ the null hypothesis was accepted verifying that the 5 datum points were stable.

The weight constraints solution based on the datum definition is presented in Table 4.

Point name	h_0 [m]	σ_{h_0} [m]	\dot{h} [m/year]	$\sigma_{\dot{h}}$ [m/year]	c [m/year]	σ_c [m/year]
LHAV	417.103	0.0031	0.0022	0.0060	-0.0868	0.0168
436A	257.172	0.0039	-0.0060	0.0080	-0.0646	0.0214
362A	-29.659	0.0030	-0.0013	0.0059	0.0127	0.0163
OFKM	48.489	0.0029	0.0007	0.0056	0.0005	0.0155
4727	183.527	0.0031	0.0028	0.0067	-0.0192	0.0178
ASHK	-186.731	0.0026	0.0013	0.0055	0.0239	0.0150
402U	-210.117	0.0040	0.0152	0.0078	-0.0551	0.0213
040F	-15.626	0.0039	-0.0034	0.0078	-0.0179	0.0203
065F	-254.655	0.0043	0.0165	0.0084	-0.0339	0.0220
718A	-285.590	0.0041	0.0119	0.0079	-0.0346	0.0213
EZRA	-175.199	0.0040	0.0189	0.0077	-0.0673	0.0210

Table 4: The weight constraints solution of the swelling and shrinking model, where points 362A, OFKM, 4727, 402U and 040F (yellow background) defined the network datum.

After setting a stable datum, a single point test was carried for all the other points in the network. If the null hypothesis was accepted for a single point then the point was considered stable at a significance level α . Otherwise a significant movement was defined for the point. Four points were found to have significantly moved (see Fig 1.); 2 points (LHAV and 436A) in the southeast part of the network and 2 points (402U and EZRA) in the center of the network near the coastline. The results of the single point testing are presents in Table 5.

Point name	h	r	$F(\alpha, h, r)$	k	Significant
LHAV	2	∞	3.0	13.96	yes
436A	2	∞	3.0	6.04	yes
402U	2	∞	3.0	4.33	yes
065F	2	∞	3.0	2.58	no
718A	2	∞	3.0	2.07	no
EZRA	2	∞	3.0	6.81	yes

Table 5: Single point testing results for a significance level $\alpha = 5\%$.

Figure 1 depicts the behavior of the tested points for the shrinking and swelling model, when compared with the datum points. The blue points represent the measured height in the 9 campaigns. The black line represents the linear trend motion and the pink line represents the swelling and shrinking model.

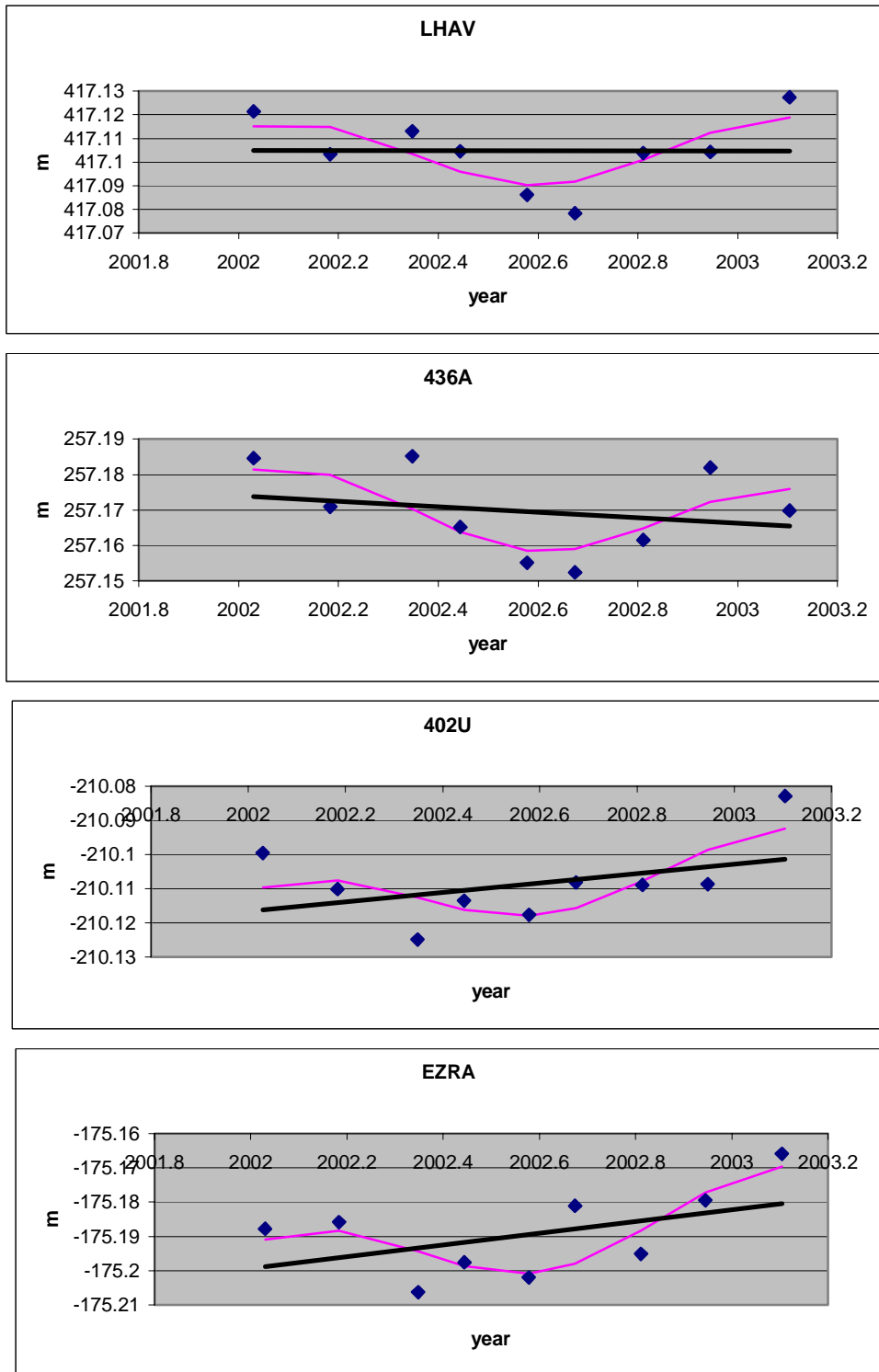


Figure 1: The swelling and shrinking model in the points with significant movement relative to the datum points (362A, OFKM, 4727, 402U, 40F).

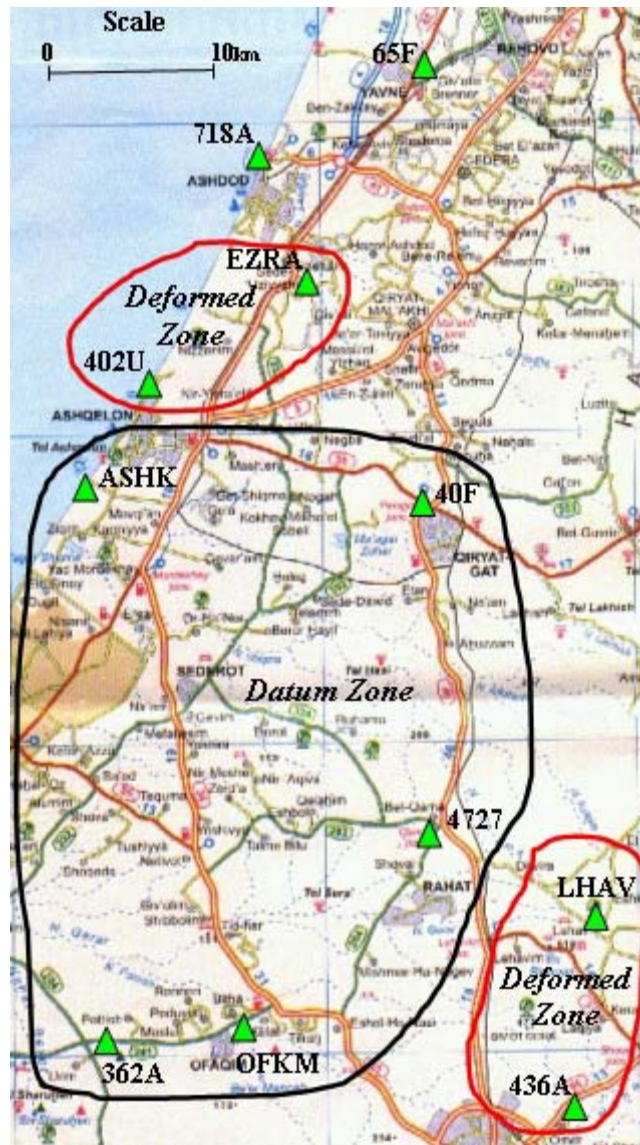


Figure 2: Map of the monitoring area. Green triangles represent monitoring network point. Black lines define the datum zone and the red line define the deformed zone

6. DISCUSSION AND CONCLUSIONS

A number of different sources may contribute to the apparent variations in the observed vertical site positions. These sources include global and local phenomenon, where the local phenomenon is divided to systematic and incidental dependant phenomenon. Therefore, the vertical position of a point may change in a constant manner, in a systematic cyclic manner, in an incidental cyclic manner or in an arbitrary manner.

Constant movement may be caused by tectonic plate movements and can be divided into constant velocity and acceleration. Cyclic movement, systematic or incidental, can be caused by physical processes of regular or irregular character like solid earth, ocean and atmospheric

tides, ground water, hydrodynamic and thermal expansion of bedrock etc. GPS measurements are characterized by some modeling errors as well, such as errors in the modeling of satellite orbit; atmospheric and water vapor modeling and antenna phase center which may have seasonal components as well.

Based on the examination of the continuous GPS array daily solutions, Dong et al. (2002) compared the relative contributions of the different sources and found that surface mass redistribution, including ocean and earth tides, as well as atmospheric and ground water loading, are the primary causes for the observed annual vertical variations of site positions. The contributions of geophysical sources and model errors to the observed annual vertical variations in site positions are in the magnitude of several millimeters.

It is logical to assume that most of the global and regional physical processes which cause instability will have the same effects in a small area. Looking at the 5 point datum defined for this research, significant shrinking and swelling movements are evident in two local areas, each defined by a pair of points. The annual amplitude of the points LHAV and 436A relative to the reference system is approximately 12mm, and for the points 402U and EZRA it is approximately 10mm. The linear motion measured for points LHAV and 436A is smaller than the motion measured for points 402U and EZRA. The larger linear motion of points 402U and EZRA may be caused by the ground water level and linear changes in the Mediterranean Sea level. These two points are close to the coastline and a Mario-graph located near to point 402U showed positive linear rising of the sea level by 13cm over the monitoring year.

Attempting to explain the variations in the position of the points by soil expansion schemes according to the rainfall cycle is complicated. The swelling and shrinking model is best fitting when defining the zero epoch t_0 as 2002.1. In this model the extreme points are received in the beginning of January and August (which in Israel mark the middle of winter and summer, respectively). The amount of precipitation over the investigated area is not constant, the rain fall varies between 250mm and 650mm. The rain fall season is limited to a period of four months (December to March). Therefore, we could expect a maximum swelling at the end of the winter when the soil is watered and maximum shrinking at the end of the summer when the soil is completely dry.

Any correlation between the points' construction and their movements is obvious apparent. Thus, the tested swelling and shrinking model may not be the best model to describe the local phenomenon in the investigated area. Further experimentation with different models may be carried with relative ease at the second step of the analysis, until a more suitable model is found to explain the phenomena detected in the measurements.

ACKNOWLEDGMENTS

The study reported in the above paper was supported by Survey of Israel.

REFERENCES

- Chen, Y.Q., Kavoureas M., Chrzanowski A., 1987, A Strategy for Detection of Outlying Observations in Measurements of High Precision. *The Canadian Surveyor*. 41:529-540.
- Cooper, M. A. R., 1987, "Control Surveys in Civil Engineering". Collins, London.
- Dong, D., Fang, P., Bock, Y., Cheng, M.K., and Miyazaki, S., 2002, Anatomy of Apparent Seasonal Variations from GPS-derived Site Position Time Series. *Journal of Geophysical Research*. 107(B4), 2075, doi:10.1029/2001JB000573
- Ethrog, U., 1991, Statistical Test of Significance for Testing Outlying Observations. *Survey Review*. 31:62-70.
- Even-Tzur, G., 2003, Variance Factor Estimation for Two-Step Analysis of Deformation Networks. *Journal of surveying engineering*. In printing.
- Hamilton, W.C., 1964, *Statistics in Physical Science*. The Ronald Press Company, New-York.
- Han, S. and Rizos, C., 1995, Selection and Scaling of Simultaneous Baselines for GPS Network Adjustment, or Correct Procedures for Processing Trivial Baselines. *Geomatics Research Australasia*. 63:51-66.
- Karcz, I., 1994, Geological Considerations in Design of the Seminal Dead Sea Rift Network. *Perelmuter Workshop on Dynamic Deformation Models*, Haifa, Israel.
- Koch, K.R., 1999, *Parameter Estimation and Hypothesis Testing in Linear Models*. Second Edition, Springer-Verlag, Berlin Heidelberg New-York.
- Papo, HB, and Perelmuter, A, 1993, Two-Step Analysis of Dynamical Networks. *Manuscripta Geodetica*, 18: 422-430.

BIOGRAPHICAL NOTES

Dr. Gilad Even-Tzur is a senior lecturer at the Technion - Israel Institute of Technology at the Faculty of Civil and Environmental Engineering. His research interests include GPS, Geodetic control networks, optimization of geodetic networks and Geodynamics.

CONTACTS

Gilad Even-Tzur
Department of Civil and Environmental Engineering
Technion – Israel Institute of Technology
Haifa 32000
ISRAEL
Tel. + 972 4 829 3459
Fax + 972 4 829 5708
Email: eventzur@tx.technion.ac.il